AIP | Journal of Applied Physics

Surface parameters determining a metal propensity for whiskers

Diana Shvydka and V. G. Karpov

Citation: Journal of Applied Physics **119**, 085301 (2016); doi: 10.1063/1.4942210
View online: http://dx.doi.org/10.1063/1.4942210
View Table of Contents: http://scitation.aip.org/content/aip/journal/jap/119/8?ver=pdfcov
Published by the AIP Publishing

Surface parameters determining a metal propensity for whiskers

Diana Shvydka[1,a)] and V. G. Karpov[2,b)]
[1]*Department of Radiation Oncology, University of Toledo Health Science Campus, Toledo, Ohio 43614, USA*
[2]*Department of Physics and Astronomy, University of Toledo, Toledo, Ohio 43606, USA*

(Received 14 January 2016; accepted 5 February 2016; published online 22 February 2016)

We consider surface parameters responsible for variations in propensity for whisker formation and growth between (1) different metals and (2) different recipes of the same metal. The former is attributed to metal surface tension, while the latter is related to the surface charge density that is sensitive to structure imperfections, stresses, contaminations, etc. We propose a figure of merit combining these two parameters that describes a metal propensity for whiskers and the relative smallness of whisker concentration. We argue that many previously observed correlations between whiskers and stresses, stress gradients, intermetallic compounds, contaminations, etc., can be attributed to the effects of the above two parameters. © *2016 AIP Publishing LLC*.
[http://dx.doi.org/10.1063/1.4942210]

I. INTRODUCTION

Metal whiskers grow on surfaces of some metals, such as technologically important tin and zinc (more examples are given in Tables I and II). They present metal filaments of high aspect ratio, up to $h/d \sim 10^4$, h and d being their height and diameter. The possibility of shorting across leads of electric equipment raises reliability concerns, especially significant for tin whiskers on soldering alloys. Comprehensive databases of information about tin and other metal whiskers are available through the Internet resources.[1,2]

A consensus is that whiskers develop via nucleation and growth.[3–6] Compared to the surface concentration of grains, their concentrations are small (say, by a factor of 10^{-3}–10^{-5}), varying exponentially between different local regions on the metal surface.[7–12] In particular, some of the nominally identical samples may exhibit no whiskers, others showing significant whisker infestations; therefore, it is practically impossible to grow or eliminate whiskers "on demand," which aggravates the reliability concerns. Whisker heights ($10^{-4} \lesssim h \lesssim 1$ cm) and diameters ($10^{-5} \lesssim d \lesssim 10^{-3}$ cm) are characterized by uncorrelated broad log-normal distributions.[13–15] A succinct summary of whisker properties was given by Davy.[9]

After about 70 years of research, the mechanism behind metal whiskers remains mysterious. One hypothesis points at the mechanical stress[4–6,16–18] relaxing during whisker growth and thus providing the necessary driving force. Local recrystallization regions[3,19,20] and intermetallic compounds[17,21,22] have been referred to as possible stress sources. On the other hand, it was inferred that the stress gradient rather than stress itself is the whisker driving force.[23–26] Unfortunately, these approaches lack predictive power, providing no estimates for whisker growth rates and parameters.

A recent electrostatic concept[27–32] attributes the whisker driving force to the electric fields, either induced by random surface imperfections (charge patches) or external. It is more quantitative, predicting whisker nucleation barrier, growth rates, and statistics vs. some material parameters, including the interfacial surface tension σ and surface charge density n, yet remains insufficiently verified.

The current understanding of metal whiskers faces two general questions: (Q1) Why some metals show stronger or weaker propensity for whisker growing, and what could be the underlying material parameters? (Q2) Metals showing a significant propensity for whiskers overall can grow them at higher or lower rates, often with poor predictability, depending on versatile factors, such as thermal cycling, relative humidity of ambient air, stress or stress gradients, surface contaminations, external electric fields, oxygen or hydrogen in the atmosphere, dislocations and grain boundaries, maybe some others. The question is whether these seemingly unrelated factors can be reduced to a single underlying physical quantity responsible for whisker nucleation and growth?

Here, we present arguments in favor of positive answers to both questions. Namely, we argue that (A1) surface tension can be a parameter discriminating between the differences in propensities for whisker growth between different metals, and (A2) the surface charge density (or, which is equivalent, its electric field strength) is a physical quantity underlying the above mentioned factors affecting whisker developments on various surfaces of the same metal.

II. CORRELATION WITH SURFACE TENSION

The interfacial surface tension is known to be important with all the nucleation phenomena,[33] and we do not see any reason of why it should be different for the case of metal whiskers. According to the classical nucleation theory, surface tension determines the nucleation barrier W of spherical

TABLE I. "Low" surface tension metals.

Metal	Bi	Cd	Ga	In	Pb	Sn	Tl	Zn
σ_0 (J/m^2)	0.5	0.68	0.77	0.63	0.56	0.67	0.56	0.58

[a)]Electronic mail: diana.shvydka@utoledo.edu
[b)]Electronic mail: victor.karpov@utoledo.edu

TABLE II. "Moderate" surface tension metals.

Metal	Ag	Al	Au	Be	Co	Cu
σ_0 (J/m^2)	1.2	1.1	1.4	1	1.5	1.5

particles. Including the external electric field, E, it is given by[33]

$$W = \frac{W_0}{(1 + E^2R^3\varepsilon/4W_0)^2}, \quad R = \frac{2\sigma}{\mu}, \quad W_0 \equiv \frac{16\pi\sigma^3}{3\mu^2}, \quad (1)$$

where W_0 and R are, respectively, the zero-field nucleation barrier and radius, μ is the difference between the chemical potentials per volume for the two phases involved, and σ is the surface tension of the interface between these phases.

In the case of strong electric fields, the above equation fails and the field induced nucleation of needle shaped metal particles takes place, for which the nucleation barrier is given by[27,34]

$$W = \frac{2}{3}\pi\sigma d_{\min}\sqrt{\frac{\pi\sigma\Lambda d_{\min}}{\varepsilon E^2}}. \quad (2)$$

Here, $\Lambda \equiv \ln(4h/d) - 7/3$, ε is the dielectric permittivity of a host in which the nucleation takes place, and $d_{\min}$ is a minimum diameter of a cylinder shaped nucleus still allowing for its metallic conductivity; $d_{\min} \lesssim 1$ nm.

In both cases of Eqs. (1) and (2), the nucleation rate exponential $\exp(-W/kT)$ increases with a decrease in σ, where k is the Boltzmann constant and T is the temperature. We compare the latter predictions with the data on surface tensions of metals in Tables I, II, and III. These data correspond to metals in contact with vacuum. All the metals are grouped by their *surface* tensions σ_0 conditionally categorized as "low" ($\sigma_0 < 1$ J/m^2), "moderate" ($1 \le \sigma_0 \le 1.5$ J/m^2), and "high" ($\sigma_0 > 1.5$ J/m^2); the recommended data for σ_0 are taken from Ref. 35.

Based on the literature data, whiskers have been observed for all the metals from Table I, with more than thousand publications on Sn whiskers, dozens on Zn, and less than dozen on other metals. Observations of whiskers for metals from Table II are not that numerous. They correspond to some special conditions, such as S rich environment for Ag, Ti rich for Al whiskers, and Rb rich for Au whiskers. Finally, metals from Table III have never shown any evidence of spontaneously growing whiskers on their surfaces. (The latter statements do not pertain to metal whiskers or wires and nanowires grown in certain chemical reactions or in the processes of metal depositions[36] under certain conditions.[2]) Altogether, these data show convincing correlation between the whisker propensity and metal surface tension.

TABLE III. "High" surface tension metals.

Metal	Mo	Nb	Ni	Pt	Re	Ta	Ti	W	Co	Cr	Fe	Zr
σ_0 (J/m^2)	2.6	2.2	1.9	1.9	2.2	2.5	1.9	2.7	2.4	2.1	2.2	1.9

A comment is in order regarding the meaning of surface tension σ in Eqs. (1) and (2), on one hand, and σ_0 in Tables I–III, on the other. Because the tabulated values represent the energies of surfaces in vacuum (we denote them as σ_0), they may differ significantly from the interfacial tensions σ corresponding to embryos nucleating in chemically similar hosts, such as a metal Sn embryo nucleating in a film of Sn oxide. The difference between σ_0 and σ can be as large as orders of magnitude.[37–40] In particular, the semi-empirical relation between the surface tensions of solid-liquid interface and σ_0 is $\sigma/\sigma_0 = 0.15 \pm 0.03$ for many different metals [see Eqs. (2) and (4) in Ref. 37 and a more recent study, Ref. 41]. Furthermore, that same relation was successfully used to describe the solid tin particles in aluminum matrix.[39]

In what follows, we use an order of magnitude relation, $\sigma/\sigma_0 \sim 0.1$ as a rough estimate of σ for all the metals. That relation enables one to consider the data in Tables I–III as predictors of whisker propensity for different metals.

III. CORRELATION WITH SURFACE CHARGES

Curiously, the concept of charge patches on metal surfaces was put forward[42,43] almost as long time ago as the first whisker observations. It was driven by the data on electron emission. There has been a considerable effort in developing the charge patch concept,[44–49] not related to metal propensity for whisker growth. According to that concept, the surface remains neutral as a whole, so that its negative and positive patch charges mutually balance each other overall, yet can create significant local effects. The characteristic patch size is assumed to be in the micron or sub-micron ranges.

As concluded in Ref. 42, variations of metal work functions of several tenths of electron-Volt can be due to metal surface organized along different Miller indices of different grains in a polycrystalline film; this is illustrated in Fig. 1. It was then noticed[27,28] that, additionally, the patch charges on imperfect metal surfaces can be due to many other factors, such as structural defects, oxide layers, grain boundaries, ionic contaminations, local stresses, and stress gradients. These factors create nonuniformities in the local density of electron states g (cm^{-3}eV^{-1}) making the electrons redistribute in order to minimize the system free energy, as illustrated in Fig. 2.

Here, we present some estimates translating the effects of latter imperfections into electrostatic parameters, the surface charge density ne and its corresponding field strength $E = 4\pi ne$. By the end of this section, we hope to convince the reader that all the major hypotheses and correlations so far established for the whisker driving force can be reduced to a single factor of high enough charge density on a metal surface.

A. Crystallites and grain boundaries

In addition to the above mentioned fact[42] that different grain orientations render surfaces with work functions different by several tenths of electron-volt, a concomitant factor is that the grain boundary caused impurity segregation[50,51] can lead to a significant charge density n_{GB} on the boundary. Assuming, as a rough estimate, $n_{GB} \sim 10^{14}$ cm^{-2} (i.e.,

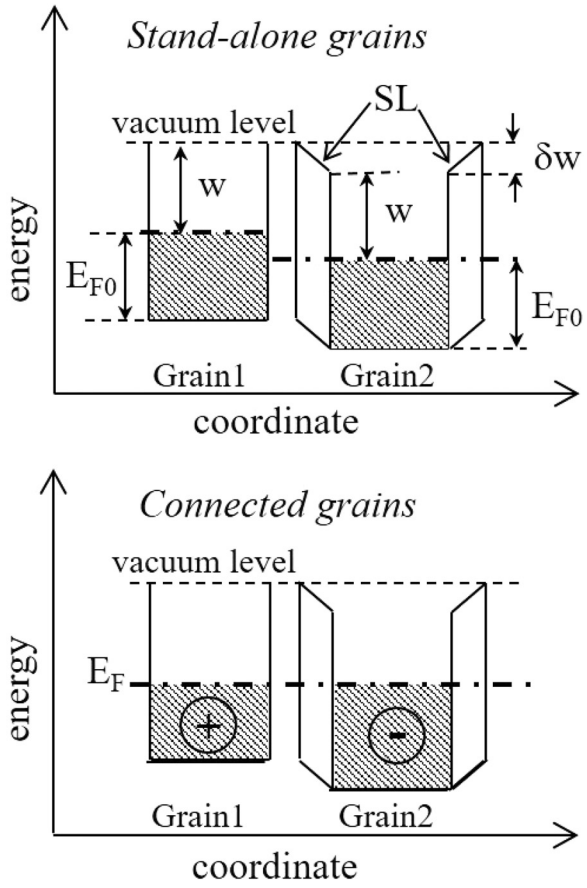

FIG. 1. *Top*: Band diagrams of two stand-alone grains, one of which has a surface layer (SL) representing chemical bonds, contaminations, etc.; w is the work function. The Fermi energies E_{F0} measured from the bottom levels, and their corresponding numbers of electrons (shaded) are the same for both grains. SL makes the energy levels in grain 2 deeper by δw than that in grain 1. *Bottom*: When the grains are electrically connected, electrons from grain 1 decrease their energies by moving to grain 2. That equalizes the Fermi levels simultaneously making grains electrically charged.

charged impurities occupying several percent of all grain boundary sites), one gets the electric potential drop $ER_s = 4\pi n_{GB} e R_s \sim 1$ V. Here, we have used the typical metal screening radius $R_s \sim 3$Å. Combining these two effects, one can expect variations of up to ~1 eV in surface energies between different grains in a polycrystalline film.

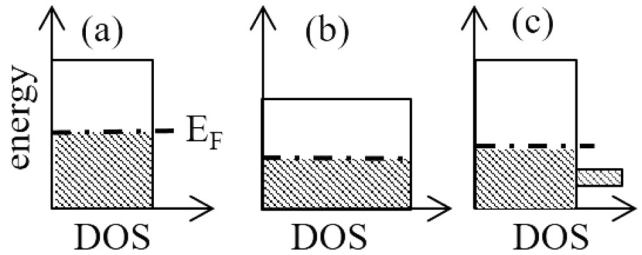

FIG. 2. Densities of electron states (DOS) represented by rectangular shapes for three grains: (a) stand-alone, (b) affected by a deformation decreasing all the energy levels, and (c) doped with impurities creating a resonance peak. The numbers of states represented by the total areas in (a) and (b) are the same, as well as the number of electrons (shaded). In (c), the number of states is greater than in (a), while the numbers of electrons are the same. Establishing electric connections ((a) and (b)) and ((a) and (c)) results in grain charging equalizing the Fermi levels.

B. Point defects and surface contaminations

Structural defects of donor or acceptor type will be screened over negligibly short distances in the depth of a metal. However, in the surface oxide or in a metal surface monolayer, their electric fields can be significant. The surface defect concentration of the order of $n \sim 10^{12}$ cm^{-2} or greater has been measured in many oxide layers.[58] A similar concentration will be generated in a surface monolayer of a metal having impurity at the level of ~10^{18} cm^{-3}, below the typical impurity concentrations in industrial metals. Assuming a single electron or hole charge per impurity atom, the corresponding field strength $E \sim 10^6$ V/cm. Note that because of the image charges in the metal, there will be surface dipoles rather than surface impurity charges. The dipoles will generate the field that is considerably lower than that due to Coulomb charges. However, rare local fluctuations in surface ion concentration will generate fields as strong as the above estimated $E \sim 10^6$ V/cm (see Sec. V for more details).

In some cases, foreign ions can change the metal density of states as illustrated in Fig. 2(c), thereby affecting the electric charge of a grain. This effect strongly depends on the host metal and impurity chemistry.

Surface contaminations of various types have been found to significantly impact metal whisker developments.[52] Attributing that effect to the electric fields,[27,28] and assuming a moderate relative ion concentration of ~0.1%, the surface density of charges can be estimated as $n \sim 10^{12}$ cm^{-2}. Taking into account again the image charges in a metal, the electric potential drop across the contaminant layer of small thickness l (illustrated as the surface layer (SL) in Fig. 1), can be estimated as $(neR^2_{\text{grain}})(l/R^2_{\text{grain}})$ where R_{grain} is the characteristic grain radius and R^2_{grain}/l represents the charge layer capacitance. Setting $n \sim 10^{12}$ cm^{-12} yields again the potential drop of the order of 1 V.

An ambient humidity is particularly important. It has been noted multiple times (see, e.g., Refs. 7–9, 53, and 54) that tin propensity for whiskers increases with the relative humidity. The interaction between water molecules and metal surfaces is complex.[55–57] Here, we limit ourselves to mentioning two effects. (i) Due to the presence of ions in relative concentrations often comparable to 0.1%, ion films on metal grains can charge the latter similarly to the above mentioned contaminants resulting in the potential drop of the order of 1 V. (ii) A near surface vapor will screen the surface field over the characteristic Debye length $R_{sD} \sim 1/\sqrt{kT/n_{\text{ion}}e^2} \sim 0.1$ μm where the ion concentration can be of the order of $n_{\text{ion}} \sim 10^{16}$ cm^{-3} (the Loschmidt number times the relative ion concentration). Given the surface electric potential, the screening will increase the field strength $E \propto 1/R_{sD}$, thereby increasing the whisker nucleation rate as more explicitly illustrated in Sec. IV.

C. Stress and stress gradients

Mechanical compressive stress once proposed to be a whisker driving force[4–6,16–18] is another source of electrostatic effects developing through the deformation potential mechanism (see, e.g., the reviews in Refs. 59 and 60).

According to that mechanism, the relative volume change $\delta V/V$ results in lowering ($D<0$) or increasing ($D>0$) of electronic energies by $D\delta V/V$, where D is the deformation potential. The corresponding change in electron concentration $\sim gD\delta V/V$ with g ($\mathrm{cm^{-3}eV^{-1}}$) being the electron density of states at the Fermi level. As a rough estimate averaging between different metals and deformations, we take $|D| \sim 3$ eV and $g \sim 10^{22}$ $\mathrm{cm^{-3}eV^{-1}}$. The relative volume change $\delta V/V \approx s/B$ can be estimated based on the published stress values,[5,6] $s \sim 20-40$ Mpa, and elastic modulus,[20] $B \sim 50-100$ GPa. Combining them yields the unbalanced electron concentration of $\sim 3\cdot(10^{17}-10^{18})$ $\mathrm{cm^{-3}}$, which, for a film of thickness $l \sim 3$ μm translates into surface charge concentration of $n \sim 10^{13}-10^{14}$ $\mathrm{cm^{-2}}$.

The latter charge concentration, while rather high, will not yet create the electric field above the perfectly flat surface or perfect spherical shell because of the system electroneutrality (meaning that there is an excessive balancing ion charges in systems of high symmetry). However, nonuniform deformations will create the net electric fields. Note in this connection that in independent experiments the field generating nonuniform deformation could be interpreted as the stress gradient effects. Consider several types of such deformations

(a) The case of quasi-spherical shell obtained by properly bending a flat structure (see, e.g., Refs. 4–6 and 23). It was shown that the assumption of perfectly spherical shells is far from reality, with deviations reaching up to 100%.[61] These deviations will translate into surface charge nonuniformities of the characteristic amplitude of $\sim nl/l_{\mathrm{sample}}$, where l and l_{sample} are, respectively, the film thickness and characteristic linear dimension of the sample. Assuming the typical $l \gtrsim 10$ μm and $l_{\mathrm{sample}} \sim 1$ cm, the latter ratio is of the order of 10^{-3}, leading to the effective surface charge densities of $n \sim 10^{11}-10^{12}$ $\mathrm{cm^{-2}}$ (sufficient for whisker nucleation as discussed in Sec. IV).

(b) The film polycrystallinity typical of whisker observations brings in the feature of local anisotropy through the elastic moduli B different for different grain orientations. The Newton's third law requires that stresses are continuous across the grain boundaries. Therefore, the strains (presented by the ratios of stress over elastic moduli) undergo significant changes, up to tens of percent, reflecting the moduli anisotropy. That leads to variations in relative volume changes, and, through the deformation potentials, to significant variations in electric charge concentration [see Fig. 2(b)]. As a result, electrons redistribute themselves nonuniformly between neighboring grains. Based on the above estimates, one can expect the surface concentration fluctuating by $n \sim 10^{12}-10^{13}$ $\mathrm{cm^{-2}}$. This interpretation can simultaneously explain the observations that stress gradients are responsible for metal whiskers.[23–26]

Note that the above discussed deformations can correspond to either compressive or tensile stresses depending on the system global conditions and local environments. For example, bending a flat structure will cause predominantly tensile or compressive stress depending on the sign of the curvature. For the case of stresses developed as a result of competition for space between individual grains in a polycrystalline film, some grains can find themselves stretched (rather than compressed) in certain random configurations where the neighboring grains are strongly compressed. The deformation potential mechanism does not favor this or other stress type, emphasizing instead spatial variations in deformation leading to near surface electric fields.

D. Intermetallic compounds and recrystallization

Once considered as whisker driving factors, the local intermetallic compounds[17,21,22] and their underlying dynamic recrystallization[3,19,20] can be linked to the electrostatic effects as well. Indeed, generally speaking, an intermetallic compound has a work function, different from that of its host by $\Delta w \sim 0.3-1$ eV, typical of the difference between work functions of two chemically different metals. Therefore, it will acquire an excessive electric charge $q \sim g\Delta weR^3$, where R is the characteristic compound radius (see Fig. 3).

If the capping layer is thin enough, $\Delta l \ll R$, then the number of charges in it becomes insufficient for complete screening, and the field penetrates outside as illustrated in Fig. 3. To estimate that field, we note that the electrons in the compound form a dipole $p \sim ql_s$ with the effective length l_s of the order of metal screening length R_s. Its field at distance r outside the metal is $E \sim qR_s/r^3$. For a numerical estimate, we use $g \sim 10^{22}$ $\mathrm{cm^{-3}eV^{-1}}$, $R_s \sim 3$Å, $r \sim R \sim 1$ μm, and $\Delta w \sim 1$ eV, which yields $E \sim 10^6$ V/cm.

In addition, since the intermetallic compound specific volume is generally different from that of host, it will create stresses, thereby contributing to the electric field as described in Sec. III C.

While a number of publications emphasize the dynamic recrystallization[3,19,20] as most significant, the approach under consideration does not account for kinetic features. We can speculate that the dynamic recrystallization passes through some configurations where the above described electric field mechanisms result in even stronger effects as being far from equilibrium.

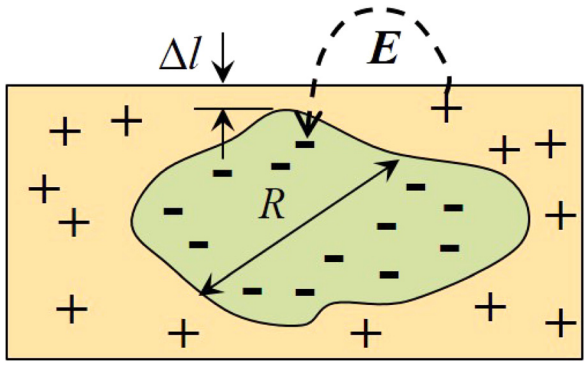

FIG. 3. A sketch of the negatively charged intermetallic compound in the host where the left behind positive charges provide the electrostatic screening. The top layer of thickness $\Delta l \ll R$ is close to depletion and does not have enough screening charges. A dashed arrow illustrates an insufficiently screened field line penetrating outside the metal layer.

E. Multi-factor effects

In some cases, several of the above factors can combine to induce a strong near-surface electric field. For example, corrosion combines a chemically different surface layer, a modified grain surface, and the corrosion related stress, all contributing to the electrostatic effects. No wonder that corrosion has been commonly referred to as a significant factor of whisker propensity.

IV. FIELD DEPENDENT WHISKER NUCLEATION

We now use the above estimates for surface tension $\sigma/\sigma_0 = 0.1$ and electric field E to predict the field effects on whisker nucleation. The nucleation time is given by

$$t = \tau_0 \exp(W/kT), \tag{3}$$

where k is the Boltzmann's constant and T is the temperature. The pre-exponential τ_0 is usually assumed to be on the order of the characteristic atomic vibration times, $\tau_0 \sim 10^{-13}$ s; its more exact estimates[33] are beyond the scope of this work. The criterion of strong field effect then becomes

$$W(0) - W(E) > kT, \tag{4}$$

where E is the external field and $W(0)$ is the nucleation barrier in zero external field. The criterion in Eq. (4) will be separately applied to Eqs. (1) and (2).

Substituting Eq. (1) into Eq. (4) yields

$$E > \sqrt{2kT/(R^3\varepsilon)} \sim 10^6 \text{V/cm}, \tag{5}$$

where we have assumed $T = 300$ K and the typical $R \sim 1$ nm, and $\varepsilon \sim 5$. This estimate does not depend on surface tension and predicts values much greater than the observed $E \sim 10^4$ V/cm, above which whisker propensity becomes dependent on the external field.[30,31]

The alternative Eq. (2) is formally unapplicable when $E = 0$. Following the electrostatic theory,[27] we assume a finite intrinsic field E_0 due to the metal imperfections, so that zero external field $E = 0$ corresponds to the barrier

$$W(0) = \frac{2}{3}\pi\sigma d_{\min}\sqrt{\frac{\pi\sigma\Lambda d_{\min}}{\varepsilon E_0^2}} \tag{6}$$

in the criterion of Eq. (4).

We start with examining the intrinsic field strength E_0 necessary for providing the observed whisker nucleation in a time $t \sim 2.5 \cdot 10^6$ s comparable to a month as often observed.[7–12] Expressing that nucleation time from Eq. (3), yields

$$E_0 = \frac{(\pi\sigma d_{\min})^{3/2} C}{kT\ln(t/\tau_0)} \quad \text{with} \quad C = \frac{2}{3}\sqrt{\frac{\Lambda}{\varepsilon}}. \tag{7}$$

With sufficient accuracy, one can set the numerical parameter $C \sim 1$. Assuming also $d_{\min} = 0.5$ nm and taking $\sigma \approx 0.07$ J/m^2, Eq. (7) yields $E_0 \sim 6 \cdot 10^5$ V/cm.

We are now in a position to estimate the external field $E(\ll E_0)$ satisfying the criterion in Eq. (4). Taking into account that $W(0) - W(E) \approx W(0)E/E_0$ and that $W(0)/kT = \ln(t/\tau_0)$, one gets

$$E \sim \frac{E_0}{\ln(t/\tau_0)} \sim 10^4 \text{V/cm}. \tag{8}$$

This estimate is in fair agreement with the data.[30,31]

Finally, we estimate the surface charge density n that is necessary to create the above field E_0. Based on the standard electrostatics, $E_0 = 4\pi ne$, which yields $n \sim 5 \cdot 10^{11}$ cm^{-2}. The latter is consistent with independent estimates from Sec. III and is within the ballpark of typical surface state densities in solids.

We conclude that the preceding analysis of interfacial tensions and surface charge density from Sections II and III leads to the correct predictions about the field effect on whisker nucleation and the density of electric charges on metal surfaces.

V. WHISKER GROWTH

In the electrostatic theory, whisker growth is determined by the competition between the surface related energy loss $F_S = \pi\sigma_0 hd$, and the electrostatic energy gain, F_E. The latter is due to interaction between the field and its induced electric dipole. Its accurate description was given in Refs. 27 and 32; here, we adopt a simple adequate approximation neglecting the field nonuniformity and allowing us to better explain the underlying physics.

Shown in Fig. 4 are three different configurations of charge patches responsible for the electric field and whisker polarization. From the standard electrostatics, a long ($h \gg L$) whisker polarization energy is determined by the charge density in the base area of radius $\rho \sim h \gg L$ (see Fig. 4). In what follows, we consider the electric field induced by different types of charge patch configurations. The major statements of this section are as follows:

A. The typical patch configurations do not favor whisker growth

Consider first the typical configuration in Fig. 4(a) with approximately equal numbers of positive and negative charges. Electric field strength is estimated as $\delta E \sim (neL^2)\delta M_0/h^2$, where neL^2 represents the absolute value of a patch charge. The induced dipole moment $p \sim \beta\delta E$ where the polarizability for a needle shaped particle is estimated as[62] $\beta \sim h^3$. The electrostatic energy, pE, then becomes

$$F_{E,\text{typ}} \sim -n^2e^2L^2h. \tag{9}$$

We compare the latter with the surface energy of a whisker

$$\frac{F_S}{|F_{E,\text{typ}}|} \sim \frac{\sigma_0 d}{n^2e^2L^2} \equiv 2\alpha. \tag{10}$$

The multiplier of 2 makes the definition of α consistent with that of our recent work.[32] α does not depend on whisker length, that is, on average, the competition between the

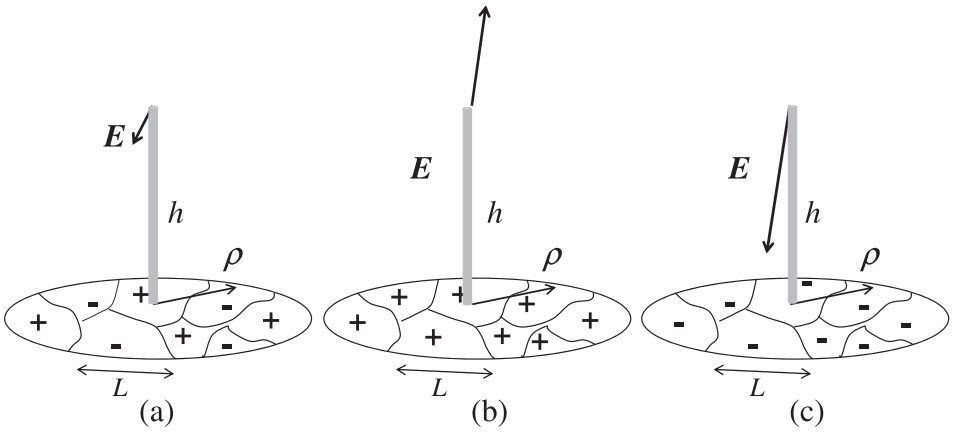

FIG. 4. (a) The typical random patch structure including approximately equal numbers of positive and negative electric charges. **E** is the electric field at the distance equal to whisker height h, and $\rho \approx h$ is the effective area contributing to the field strength E. (b) Untypical configuration dominated by the positively charged patches. (c) Untypical configuration dominated by the negatively charged patches.

whisker surface and electrostatic energies remains the same for all lengths.

Furthermore, using the standard parameters, such as $n \lesssim 10^{12}$ cm^{-2}, $L \sim d \sim 1$ μm, and $\sigma_0 \sim 1$ J/m^2, or somewhat different, it is straightforward to see that $\alpha > 1$. Therefore, the typical patch configurations does not favor whisker growth. (Note parenthetically that they can still be favorable for whisker nucleation resulting in some nodule features observed.)

B. Rare untypical configurations of charge patches give rise to metal whiskers

Consider untypical configurations where the fluctuation electric field is greater than its rms value. They are illustrated in Figs. 4(a) and 4(b) where the whisker raises from the area strongly dominated by either negative or positive charge. The free energy can be estimated as

$$F \sim \sigma_0 \pi h d - E^2 h^3, \tag{11}$$

where

$$E \sim \frac{\delta M (neL^2)}{h^2}, \tag{12}$$

where δM is the excess number of the same polarity patches in the area h^2, which is greater than its typical rms value, $\delta M (> \delta M_0)$. Assuming the uncorrelated patch distribution, the probability density of finding such a configuration is Gaussian, i.e.,

$$p(\delta M) \propto \exp\left[-\frac{(\delta M)^2}{2(\delta M_0)^2}\right]. \tag{13}$$

The minimum electric field, $E \sim \sigma_0 \pi d/h^2$ sufficient to hold a whisker of length h, is found from Eq. (11) with $F = 0$. Using it with Eq. (12) gives the minimum δM, substituting which into Eq. (13) yields the probability of finding a stable whisker

$$P \propto \exp(-\alpha). \tag{14}$$

Since $\alpha \gg 1$, the latter result shows how whisker concentration is exponentially lower than that of charge patches and their constituting crystal grains. For example, taking $\alpha \sim 10$ predicts the whisker concentration by roughly four orders of magnitude lower than that of grains, more or less consistent with the observations.

Another important conclusion is that α is a dimensionless figure of merit determining the metal whisker concentration and combining both the surface tension and charge density motifs. Since α appears in the exponent, the whisker propensity is *exponential* in both surface tension and charge density. That may explain the observed significant differences in whisker propensities between different metals and metal recipes.

A related prediction is that the majority of nuclei cannot develop into long ($h \gg L$) whiskers because they do not belong to the required charge patch configurations. We speculate that some of such nuclei reveal themselves as nodules, only a small part of which eventually transforms into whiskers, which is consistent with observations.[65]

Finally, we note that Eqs. (11) and (12) present rough approximations. In particular, their accuracy is insufficient to catch logarithmic multipliers. The technique presented in a recent publication,[32] while less physically transparent, enables one to maintain the logarithmic accuracy; it gives, instead of Eq. (14), the following result for cumulative probability:

$$W = \frac{z^{7/2}}{4\pi\alpha^2}\exp\left(-\frac{\alpha}{z}\right), \quad z \equiv \ln(h/4L). \tag{15}$$

Equation (15) leads to the log-normal type of probability density consistent with the experimental data.[32]

VI. CONCLUSIONS

A. General statement

This paper attempts a "big picture" approach to metal whiskers trying to answer a fundamental question: which parameters of metals make them so different in their propensities for whisker development. Our analysis reveals two such parameters: surface tension and surface charge density.

To avoid any misunderstanding, our findings do not question many previously established useful correlations between whiskers and stresses, stress gradients, contaminations, etc.; we just claim that those correlation can be

reduced to the effects of the above two parameters. More specifically, we have found:

(1) There exists a correlation between the surface tension and whisker nucleation/growth rate allowing to break the entire multitude of metals into three groups according to their surface energies: strong whisker growers, moderate whisker growers, and whisker resistant.
(2) We have shown that various suggested scenarios of whisker developments based on stress, polycrystallinity, contaminations, etc., can be reduced to a single physical factor of the surface electric field generated by surface imperfections. We have estimated the characteristic surface charge densities and surface fields showing that in all cases they fall in certain intervals of $n \sim 10^{11} - 10^{12}$ cm^{-2} and $E \sim 10^5 - 10^6$ V/cm.
(3) We have determined the dimensionless figure of merit α [see Eq. (10)] combining the above two material parameters and expressing a metal propensity for whiskers.
(4) We have shown that whisker concentration is exponential in α and is small compared to the surface grain concentration. This is consistent with the data, explains the observed whisker statistics and drastic differences between metals with regard to their propensity for whiskers.

B. Practical implications

(1) Because there is a general positive correlation between low melting temperatures and low surface energies (see, e.g., Ref. 63, p. 118 and Ref. 64, p. 253), our established correlation with surface tension predicts that good (low melting temperature) solders should be generally prone to whiskering.
(2) The concept that surface charge density is a factor behind a propensity for whiskering suggests a natural antidote in the form of neutralizing surface charges, such that the excessive negative local charge density is balanced by intentionally added positive ions and vice versa. These treatments can be self-healing in a process where some extraneous ions possess enough motility to drift towards the oppositely charged region on the surface; an example of such self-healing treatment is known, e.g., in photovoltaics.[66,67]

ACKNOWLEDGMENTS

This work was partially supported by the NRC faculty development Grant No. NRC-HQ-12-G-38-0042. We acknowledge fruitful discussions with the University of Toledo whisker group members (D. Georgiev, R. Irving, C. Grice, V. Borra, G. Warrell, and D. Niraula) and very stimulating insights from the members of Bill Rollins' Tin Whisker Teleconference group.[2]

[1]See http://nepp.nasa.gov/whisker for NASA Goddard space flight center tin whisker homepage.
[2]J. R. Barnes, see http://www.dbicorporation.com/whiskbib.htm for bibliography for tin whiskers, zinc whiskers, cadmium whiskers, indium whiskers, and other conductive metal and semiconductor whiskers.

[3]J. Cheng, P. T. Vianco, B. Zhang, and J. C. M. Li, "Nucleation and growth of tin whiskers," Appl. Phys. Lett. **98**, 241910 (2011).
[4]F. Pei and E. Chason, "In situ measurement of stress and whisker/hillock density during thermal cycling of Sn layers," J. Electron. Mater. **43**, 80 (2014).
[5]E. Chason, F. Pei, C. L. Briant, H. Kesari, and A. F. Bower, "Significance of nucleation kinetics in Sn whisker formation," J. Electron. Mater. **43**, 4435 (2014).
[6]F. Pei, C. L. Briant, H. Kesari, A. F. Bower, and E. Chason, "Kinetics of Sn whisker nucleation using thermally induced stress," Scr. Mater. **93**, 16 (2014).
[7]G. T. Galyon, "Annotated tin whisker bibliography and anthology," IEEE Trans. Electron. Packag. Manuf. **28**, 94 (2005).
[8]J. Brusse, G. Ewell, and J. Siplon, "Tin whiskers: Attributes and mitigation," *Capacitor and Resistor Technology Symposium (CARTS)*, March 25–29, 2000, pp. 68–80.
[9]G. Davy, private communication (10 October 2014).
[10]Y. Zhang, "Tin whisker discovery and research," in *Soldering in Electronics*, edited by K. Suganuma (Marcel Dekker, Inc., 2004), p. 121.
[11]K. N. Tu, J. O. Suh, and A. T. Wu, "Tin whisker growth on lead-free solder finishes," in *Lead-Free Solder Interconnect Reliability*, edited by D. Shangguan (ASM International, 2005), p. 851.
[12]D. Bunyan, M. A. Ashworth, G. D. Wilcox, R. L. Higginson, R. J. Heath, and C. Liu, "Tin whisker growth from electroplated finishes a review," Trans. Inst. Met. Finish. **91**, 249–259 (2013).
[13]T. Fang, M. Osterman, and M. Pecht, "Statistical analysis of tin whisker growth," Microelectron. Reliab. **46**, 846 (2006).
[14]L. Panashchenko, "Evaluation of environmental tests for tin whisker assessment," M.S. thesis, University of Maryland, 2009; URL:http://hdl.handle.net/1903/10021.
[15]D. Susan, J. Michael, R. P. Grant, B. McKenzie, and W. G. Yelton, "Morphology and growth kinetics of straight and kinked tin whiskers," Metall. Mater. Trans. A **44**, 1485 (2013).
[16]W. J. Boettinger, C. E. Johnson, L. A. Bendersky, K.-W. Moon, M. E. Williams, and G. R. Stafford, "Whisker and hillock formation on Sn, SnCu, and SnPb electrodeposits," Acta Mater. **53**, 5033 (2005).
[17]N. Jadhav, E. J. Buchovecky, L. Reinbold, S. Kumar, A. F. Bower, and E. Chason, "Understanding the correlation between intermetallic growth, stress evolution, and Sn whisker nucleation," IEEE Trans. Electron. Packag. Manuf. **33**, 183 (2010).
[18]P. Sarobol, J. E. Blendell, and C. A. Handwerker, "Whisker and hillock growth via coupled localized Coble creep, grain boundary sliding, and shear induced grain boundary migration," Acta Mater. **61**, 1991 (2013).
[19]P. Vianco, M. Neilsen, J. Rejent, and R. Grant, "Validation of the dynamic recrystallization (DRX) mechanism for whisker and hillock growth on Sn thin films," J. Electron. Mater. **44**, 4012 (2015).
[20]L. Qiang and Z. Huang, "A physical model and analysis for whisker growth caused by chemical intermetallic reaction," Microelectron. Reliab. **54**, 2494 (2014).
[21]K. N. Tu, "Irreversible processes of spontaneous whisker growth in bimetallic Cu-Sn thin-film reactions," Phys. Rev. B **49**, 2030 (1994).
[22]A. C. K. So and Y. C. Chan, "Reliability studies of surface mount solder joints effect of Cu-Sn intermetallic compounds," IEEE Trans. Compon. Packag. Manuf. Technol. Part B **19**, 661 (1996).
[23]J. Stein, M. Pascher, U. Welzel, W. Huegel, and E. J. Mittemeijer, "Imposition of defined states of stress on thin films by a wafer-curvature method; validation and application to aging Sn films," Thin Solid Films **568**, 52 (2014).
[24]F. Yang and Y. Li, "Indentation-induced tin whiskers on electroplated tin coatings," J. Appl. Phys. **104**, 113512 (2008).
[25]M. Sobiech, U. Welzel, E. J. Mittemeijer, W. Hugel, and A. Seekamp, Appl. Phys. Lett. **93**, 011906 (2008).
[26]M. Sobiech, M. Wohlschlgel, U. Welzel, E. J. Mittemeijer, W. Hugel, A. Seekamp, W. Liu, and G. E. Ice, "Local, submicron, strain gradients as the cause of Sn whisker growth," Appl. Phys. Lett. **94**, 221901 (2009).
[27]V. G. Karpov, "Electrostatic theory of metal whsikers," Phys. Rev. Appl. **1**, 044001 (2014).
[28]V. G. Karpov, Electrostatic Mechanism of Nucleation and Growth of Metal Whiskers, SMT Magazine, February 2015, p. 28.
[29]V. G. Karpov, "Understanding the movements of metal whiskers," J. Appl. Phys. **117**, 235303 (2015).
[30]A. C. Vasko, G. R. Warrell, E. I. Parsai, V. G. Karpov, and D. Shvydka, "Electron beam induced growth of tin whiskers," J. Appl. Phys. **118**, 125301 (2015).

[31]A. C. Vasko, C. R. Grice, A. D. Kostic, and V. G. Karpov, in Evidence of Electric-field-Accelerated Growth of Tin Whiskers, MRS Communications (Mater. Res. Soc. Symp. Proc., 2015).
[32]D. Niraula and V. G. Karpov, "The probabilistic distribution of metal whisker lengths," J. Appl. Phys. **118**, 205301 (2015).
[33]D. Kaschiev, *Nucleation: Basic Theory with Applications* (Butterworth-Heinemann, Oxford, Amsterdam, 2000).
[34]V. G. Karpov, Y. A. Kryukov, I. V. Karpov, and M. Mitra, "Field induced nucleation in glasses," Phys. Rev. B **78**, 052201 (2008).
[35]V. K. Kumikov and Kh. B. Khokonov, "On the measurement of surface free energy and surface tension of solid metals," J. Appl. Phys. **54**, 1346 (1983).
[36]G. Richter, K. Hillerich, U. D. S. Gianola, R. Monig, O. Kraft, and C. A. Volkert, "Ultrahigh strength single crystalline nanowhiskers grown by physical vapor deposition," Nano Lett. **9**, 3048 (2009).
[37]W. R. Tyson and W. A. Miller, "Surface free energies of solid metals: Estimation from liquid surface tension measurements," Surf. Sci. **62**, 267 (1977).
[38]U. O. M. Vazquez, W. Shinoda, P. B. Moore, C. Chiu, and S. O. Nielsen, "Calculating the surface tension between a flat solid and a liquid: A theoretical and computer simulation study of three topologically different methods," J. Math. Chem. **45**, 161 (2009).
[39]W. T. Kim and B. Cantor, "Solidification of tin droplets embedded in an aluminium matrix," J. Mater. Sci. **26**, 2868 (1991).
[40]B. Yang, A. S. Abyzov, E. Zhuravlev, Y. Gao, J. W. P. Schmelzer, and C. Schick, "Size and rate dependence of crystal nucleation in single tin drops by fast scanning calorimetry," J. Chem. Phys. **138**, 054501 (2013).
[41]B. Vineti, L. Magnusson, H. Fredriksson, and P. J. Disre, "Correlations between surface and interface energies with respect to crystal nucleation," J. Colloid Interface Sci. **255**, 363 (2002).
[42]C. Herring and M. H. Nichols, "Thermoionic emission," Rev. Mod. Phys. **21**, 185 (1949).
[43]M. S. Rzchowski and J. R. Henderson, "Properties of random fields outside a metal surface and their effect on time-of-flight spectroscopy," Phys. Rev. A **38**, 4622 (1988).
[44]J. B. Camp, T. W. Darling, and R. E. Brown, "Macroscopic variations of surface potentials of conductors," J. Appl. Phys. **69**, 7126 (1991).
[45]E. Bano, T. Ouisse, L. Di Cioccio, and S. Karmann, "Surface potential fluctuations in metaloxide semiconductor capacitors fabricated on different silicon carbide polytypes," Appl. Phys. Lett. **65**, 2723 (1994).
[46]J. Labaziewicz, Y. F. Ge, D. R. Leibrandt, S. X. Wang, R. Shewmon, and I. L. Chuang, "Temperature dependence of electric field noise above gold surfaces," Phys. Rev. Lett. **101**, 180602 (2008).
[47]R. Dubessy, T. Coudreau, and L. Guidoni, "Electric field noise above surfaces: A model for heating-rate scaling law in ion traps," Phys. Rev. A **80**, 031402R (2009).
[48]G. H. Low, P. F. Herskind, and I. L. Chuang, "Finite geometry models of electric field noise from patch potentials in ion traps," Phys. Rev. A **84**, 053425 (2011).
[49]J. L. Garrett, D. Somers, and J. N. Munday, "The effect of patch potentials in Casimir force measurements determined by heterodyne Kelvin probe force microscopy," J. Phys.: Condens. Matter **27**, 214012 (2015).
[50]P. Lejcek, *Grain Boundary Segregation in Metals*, Springer Series in Materials Science (Springer, 2010).
[51]G.-H. Lu, A. Suzuki, A. Ito, M. Kohyama, and R. Yamamoto, "Effects of impurities on an Al grain boundary," Mater. Trans. **44**, 337 (2003).
[52]T. Munson and P. Solis, Metal Whiskers Does Surface Contamination Have an Effect of Whisker Formation?, http://www.ipcoutlook.org/pdf/metal_whiskers_does_surface_contamination_ipc.pdf.
[53]A.-P. Xiana and M. Liua, "Effect of humidity on tin whisker growth from Sn3Nd intermetallic compound," J. Mater. Res. **27**, 1652 (2012).
[54]C.-F. Li, Z.-Q. Liu, and J.-K. Shang, "The effects of temperature and humidity on the growth of tin whisker and hillock from Sn5Nd alloy," J. Alloys Compd. **550**, 231 (2013).
[55]A. Hodgson and S. Haq, "Water adsorption and the wetting of metal surfaces," Surf. Sci. Rep. **64**, 381 (2009).
[56]J. Carrasco, A. Hodgson, and A. Michaelides, "A molecular perspective of water at metal interfaces," Nature Mater. **11**, 667 (2012).
[57]A. J. Barthel and S. H. Kim, "Surface chemistry dependence of water adsorption on solid substrates in humid ambient and humidity effects on wear of copper and glass surfaces," Tribology **7**, 23 (2013).
[58]S. M. Sze, *Physics of Semiconductor Devices* (Wiley, New York, 1981).
[59]G. Grimvall, *The Electron-Phonon Interaction in Metals* (North Holland, Amsterdam, 1981).
[60]J. Kruger, "Electron-phonon coupling at metal surfaces," Rep. Prog. Phys. **69**, 899 (2006).
[61]M. R. Ardigo, M. Ahmed, and A. Besnard, "Stoney formula: Investigation of curvature measurements by optical profilometer," Adv. Mater. Res. **996**, 361 (2014).
[62]L. D. Landau, I. M. Lifshitz, and L. P. Pitaevskii, *Electrodynamics of Continuous Media* (Pergamon, Oxford, New York, 1984).
[63]D. A. Porter, K. E. Easterling, and M. Y. Sherif, *Phase Transformations in Metals and Alloys*, 3rd ed. (CRC Press, Taylor and Francis, Boca Raton, 2009).
[64]R. Asthana, A. Kumar, and N. B. Dahotre, *Materials Processing and Manufacturing Science* (Elsevier, Amsterdam, 2006).
[65]K. Murakami1, M. Okano, M. Hino, M. Takamizawa, and K. Nakai, "Mechanism of generation and suppression of tin whiskers on tin and tin-lead plated films," Mater. Trans. **51**, 143 (2010).
[66]V. G. Karpov, Y. Roussillon, D. Shvydka, A. D. Compaan, and D. M. Giolando, "Photovoltaic healing of nonuniformities in semiconductor devices," U.S. patent 7,098,058 B1 (29 August 2006).
[67]Y. Roussillon, D. Giolando, D. Shvydka, A. D. Compaan, and V. G. Karpov, "Blocking thin film nonuniformities: Photovoltaic self-healing," Appl. Phys. Lett. **84**, 616 (2004).